New Astronomy 29 (2014) 42–46

Contents lists available at ScienceDirect

New Astronomy

journal homepage: www.elsevier.com/locate/newast

Photoionization of fine structure levels of Ne IV

Sultana N. Nahar *

Department of Astronomy, The Ohio State University, Columbus, OH 43210, United States

HIGHLIGHTS

- Ne IV photoionization cross sections are important to study the spectral lines in planetary nebulae, supernova SN1987 etc.
- Present study include relativistic effects not considered earlier and new features are seen.
- Relativistic couplings introduce new and important near threshold resonances that will affect recombination, photoionization rates.
- Photoionization of many excited levels are considered for modeling.
- Fine structure couplings give more and higher resolution resonances with increased accuracy.

ARTICLE INFO

Article history:
Received 21 November 2013
Received in revised form 5 December 2013
Accepted 8 December 2013
Available online 14 December 2013
Communicated by G.F Gilmore

Keywords:
Photoionization Ne IV
Cross sections for many excited levels
Relativistic Breit–Pauli calculations
Atomic spectra 32.10-f, 95.30.Ky, 32.80-t

ABSTRACT

Study of characteristic features in photoionization of a large number of excited levels of Ne IV, ($h\nu$ + Ne IV → Ne V + e), using ab initio Breit–Pauli R-matrix (BPRM) method, is presented. This is the second large atomic system, after Fe XVII, for which BPRM method has been used for a full scale computation of photoionization cross sections for a large number of bound levels ($N \leqslant 10$). The study include features, such as, of Seaton resonances due to photo-excitation-of-core and new near threshold resonant features. Coupling of fine structure channels due to relativistic effects is found to introduce low energy resonances near threshold, not allowed in LS coupling approximation. These resonances play crucial role for low temperature recombination rates. Photoionization cross sections (σ_{PI}) for the largest set of levels of Ne IV, a total of 868, with $n \leqslant 10$ and $l \leqslant 9$ are presented. A wave function expansion optimized with 24 configurations with orbitals going up to 4p of core Ne V was used. Resonances due to Rydberg series of autoionizing states belonging to various core excited core levels are resolved with fine energy mesh. Details of resonant structures and enhanced background due to Seaton resonances are elaborated in this first study of the ion with relativistic effects.

1. Introduction

Neon ions are known to exist in many astronomical objects (e.g. Houck et al., 2004). Being present in the nebular gas, such as in Orion, where new stars are born and in planetary nebulae which is the end point of a star, lines of Ne IV provides information of the chronometer of the universe. Lines of the ion in ultra luminous infrared galaxies (ULIRG) are related to chemical evolution of galaxies. However, due to lack of high accuracy atomic data discrepancy remains between the observed and theoretically predicted values. For example, the diagnostic line ratio 14/24 in μm of Ne V due to collision is found to be lying below the theoretical low density limit (Rubin et al., 2001; Rubin, 2004).

Photoionization of Ne IV is investigated under the Iron Project (Hummer et al., 1993) for high accuracy atomic data for collisional (Dance et al., 2013) and radiative processes (e.g. for radiative transitions Nahar, 2013) with inclusion of relativistic effects. Breit–Pauli R-matrix (BPRM) method was developed under the IP about two decades ago. However, because of computational challenges and complexity of spectroscopic identification of fine structure levels, the method has been used for photoionization cross sections of a very limited number of ions and most of the results are only for a few low-lying levels. The existing full scale calculations for a large number of bound levels are available for He- and Li-like ions (e.g. Nahar, 2013). The only large atomic system for which the BPRM method was used for photoionization cross sections of levels $n \leqslant 10$ is for neon like, Fe XVII, (Nahar et al., 2011). Full scale data are needed for various astrophysical and laboratory applications. The present study reports photoionization of Ne IV of a large number of excited levels with detailed features. Computation with relativistic effects increases considerably as the number of fine structure levels increases from LS terms and finer energy mesh is required for resolution of larger number of Rydberg series of narrow resonances by fine structure splitting of core excitations. The

* Tel.: +1 614 292 1888; fax: +1 614 292 2928.
E-mail address: nahar@astronomy.ohio-state.edu
URL: http://www.astronomy.ohio-state.edu/~nahar

1384-1076/$ - see front matter © 2013 Elsevier B.V. All rights reserved.
http://dx.doi.org/10.1016/j.newast.2013.12.001

major complexity arises from spectroscopic designation of the large number of un-identified fine structure levels that are computed from the Hamiltonian in BPRM method. This has limited the use of BPRM method largely to photoionization of He- and Li-like ions (e.g. Nahar, 2013).

The earlier detailed work on Ne IV photoionization cross sections were obtained under the Opacity Project (1995) by Lennon et al. (1993). Although the work was not published, the data are available through OP database TOPbase. They used non-relativistic R-matrix method and considered lower number of states.

2. Theory and computations

Photoionization occurs directly,

$$h\nu + X^+ \rightarrow e + X^{++}, \tag{1}$$

as well as through an intermediate doubly excited autoionization state

$$e + X^{++} \leftrightharpoons (X^+)^{**} \leftrightharpoons \begin{cases} (a)\ e + X^{++}(AI) \\ (b)\ h\nu + X^+(DR) \end{cases} \tag{2}$$

where the intermediate doubly excited autoionizing state leads either to autoionization (AI) where the electron goes free or to dielectronic recombination (DR) where the electron is captured by emission of a photon. An autoionizing state introduce a resonance which can be obtained theoretically by including the core excitations in the wave function, as considered in close coupling (CC) approximation. The CC approximation the atomic system is represented by a 'target' or the 'core' ion of N-electrons system interacting with the (N + 1)th electron. The (N + 1)th electron is bound or in the continuum depending on its negative or positive energy (E). The total wave function, Ψ_E, of the (N + 1) electrons system in a symmetry $SL\pi$ is represented by an expansion as

$$\Psi_E(e + ion) = A\sum_i \chi_i(ion)\,\theta_i + \sum_j c_j \Phi_j, \tag{3}$$

where the target ion eigenfunction, χ_i, is coupled with the (N + 1)th electron function, θ_i. The sum is over the ground and excited core states. The (N + 1)th electron with kinetic energy k_i^2 is in a channel labeled as $S_iL_i\pi_i k_i^2 \ell_i\,(SL\pi)$. In the second sum, the Φ_js are bound channel functions of the (N + 1)-electrons system that account for short range correlation and the orthogonality between the continuum and the bound electron orbitals. Substitution of $\Psi_E(e + ion)$ in the Schrodinger equation

$$H_{N+1}\Psi_E = E\Psi_E \tag{4}$$

introduces a set of coupled equations that are solved using the R-matrix approach.

The details of the R-matrix method in the CC approximation can be found in, e.g. Burke and Robb (1975), Seaton (1987), Berrington et al. (1987), Berrington et al. (1995) and Pradhan and Nahar (2011). The relativistic effects are included through Breit–Pauli approximation (e.g. Pradhan and Nahar, 2011). The Hamiltonian of the (N + 1)-electrons system in the Breit–Pauli R-matrix (BPRM) method is given by Hummer et al. (1993) and Pradhan and Nahar (2011)

$$H_{N+1}^{\rm BP} = \sum_{i=1}^{N+1}\left\{-\nabla_i^2 - \frac{2Z}{r_i} + \sum_{j>i}^{N+1}\frac{2}{r_{ij}}\right\} + H_{N+1}^{\rm mass} + H_{N+1}^{\rm Dar} + H_{N+1}^{\rm so}, \tag{5}$$

where Rydberg unit (1/2 of Hartree) has been used. The additional terms are relativistic one-body correction terms, the mass correction, $H^{\rm mass} = -\frac{\alpha^2}{4}\sum_i p_i^4$, Darwin, $H^{\rm Dar} = \frac{Z\alpha^2}{4}\sum_i \nabla^2\left(\frac{1}{r_i}\right)$, and the spin–orbit interaction, $H^{\rm so} = Z\alpha^2\sum_i \frac{1}{r_i^3}\mathbf{l_i}\cdot\mathbf{s_i}$. BPRM includes these and part of two-body interaction terms, such as the ones without the momentum operators (Pradhan and Nahar, 2011). In BPRM method. the set of $SL\pi$ is recoupled for $J\pi$ levels of (e + ion) system which is followed by diagonalization of the Hamiltonian. The solution is a continuum wave function, Ψ_F, for an electron with positive energies ($E > 0$), or a bound state, Ψ_B, at a negative total energy ($E \leqslant 0$). The complex resonant structures in photoionization result from channel couplings between continuum channels that are open ($k_i^2 > 0$), and ones that are closed ($k_i^2 < 0$), at electron energies k_i^2 corresponding to autoionizing states of the Rydberg series, $S_iL_iJ_i\pi_i\nu\ell$ where ν is the effective quantum number, converging to the target thresholds.

Transition matrix elements for photoionization, $< \Psi_B||\mathbf{D}||\Psi_F >$ where $\mathbf{D} = \sum_i \mathbf{r}_i$ is the dipole operator and the sum is over the number of electrons, are obtained from the bound and continuum wave functions. The transition matrix element can be reduced to generalized line strength as

$$\mathbf{S} = |< \Psi_j||\mathbf{D}_L||\Psi_i >|^2 = \left|\left\langle \psi_f \mid \sum_{j=1}^{N+1} r_j \mid \psi_i \right\rangle\right|^2, \tag{6}$$

where Ψ_i and Ψ_f are the initial and final state wave functions. The photoionization cross section (σ_{PI}) is proportional to the generalized line strength as,

$$\sigma_{PI} = \frac{4\pi^2}{3c}\frac{1}{g_i}\omega\mathbf{S}, \tag{7}$$

where g_i is the statistical weight factor of the bound state and ω is the incident photon energy. Although radiation damping of the resonances is included (Zhang et al., 1999), it is not important for this ion.

3. Computation

BPRM calculations are initiated with the wave function of the core as the input. These core wave functions are typically obtained from optimized atomic structure calculations. The wave function of core Ne V was obtained by optimization of the ground and 24 excited configurations as listed in Table 1 using the later version (Nahar et al., 2003) of atomic structure code SUPERSTRUCTURE (SS) (Eissner et al., 1974). SS which uses Thomas–Fermi approximation includes relativistic contributions in Breit–Pauli approximation in the later version. Table 1 presents the Thomas–Fermi scaling parameters for the orbitals. Twenty fine structure levels of Ne V of configurations $1s^22s^22p^2$, $1s^22s2p^3$, $1s^22p^4$, listed in Table 1, were considered in the R-matrix calculations. Both the calculated and observed (NIST) level energies are given in Table 1. Comparison shows that except for the $1s^22s^22p^2(^1D)$ and $1s^22s2p^3(^5S^0_2)$ levels, the calculated energies agree very well with the observed values listed in compiled table at NIST.[1] No observed values are available for levels $1s^22p^4(^1D)$ and $1s^22p^4(^1S)$. Except for these two levels. the observed energies were used in the calculations as they provide more accurate resonance positions.

The interacting electron partial wave expansion are specified for $0 \leqslant \ell \leqslant 14$, with a R-matrix basis set of 15 continuum functions. The R-matrix boundary was chosen to be large enough, 9 a_o, to accommodate the bound orbitals. The second term of the wave function in Eq. (3), which represents the bound state correlation functions, includes 76 $(N + 1)$-particle configurations with orbital occupancies from minimum to a maximum number as given within parentheses of the orbitals 1s(2-2), 2s(0-2), 2p(0-5), 3s(0-2), 3p(0-3), 3d(0-2), 4s(0-2), 4p(0-2). Computations are carried out for all angular momenta, $0 \leqslant L \leqslant 12$, $1/2 \leqslant J \leqslant 21/2$.

Photoionization cross sections are obtained with consideration of radiation damping for all bound levels using the BPRM R-matrix

[1] <http://physics.nist.gov/PhysRefData/ASD/levelsform.html>.

Table 1
Levels and energies (E_t) of target (core ion) Ne V in wave function expansion of Ne IV. They were optimized using a set of 24 spectroscopic configurations: $2s^22p^2(1)$, $2s2p^3(2)$, $2s^22p3s(3)$, $2p^4(4)$, $2s^22p3p(5)$, $2s^22p3d(6)$, $2s^22p4s(7)$, $2s^22p4p(8)$, $2s2p^23s(9)$, $2s2p^23p(10)$, $2s2p^23d(11)$, $2s^23s^2(12)$, $2s^23p^2(13)$, $2s^23d^2(14)$, $2s^24s^2(15)$, $2s^24p^2(16)$, $2s^23s3p(17)$, $2s^23s3d(18)$, $2s^23s4s(19)$, $2s^23s4p(20)$, $2s^23p3d(21)$, $2p^33s(22)$, $2p^33p(23)$, $2p^33d(24)$ with filled 1s orbital. The Thomas–Fermi scaling parameters for the orbitals are 1.47637(1s), 1.47637(2s), 1.27184(2p), 1.47637(3s), 1.27184(3p), 1.19306(3d), 1.47637(4s), 1.27184(4p). The present calculated energies (SS) are compared with the observed energies listed in the NIST table of compilation.

	Level	J_t	E_t(Ry) NIST	E_t(Ry) SS
1	$1s^22s^22p^2(^3P)$	0	0.0	0.
2	$1s^22s^22p^2(^3P)$	1	0.003758	0.0030391
3	$1s^22s^22p^2(^3P)$	2	0.010116	0.011366
4	$1s^22s^22p^2(^1D)$	2	0.276036	0.30391
5	$1s^22s^22p^2(^1S)$	2	0.582424	0.57413
6	$1s^22s2p^3(^5S^o)$	2	0.8052	0.71604
7	$1s^22s2p^3(^3D^o)$	3	1.60232	1.62957
8	$1s^22s2p^3(^3D^o)$	2	1.60296	1.62932
9	$1s^22s2p^3(^3D^o)$	1	1.60316	1.62929
10	$1s^22s2p^3(^3P^o)$	2	1.89687	1.92363
11	$1s^22s2p^3(^3P^o)$	1	1.89687	1.92340
12	$1s^22s2p^3(^3P^o)$	0	1.89719	1.92328
13	$1s^22s2p^3(^1D^o)$	2	2.46556	2.59326
14	$1s^22s2p^3(^3S^o)$	1	2.54576	2.64956
15	$1s^22s2p^3(^1P^o)$	1	2.76854	2.88988
16	$1s^22p^4(^3P)$	2	3.76063	3.86076
17	$1s^22p^4(^3P)$	1	3.76778	3.86807
18	$1s^22p^4(^3P)$	0	3.77085	3.87155
19	$1s^22p^4(^1D)$	2		4.13816
20	$1s^22p^4(^1S)$	0		4.74472

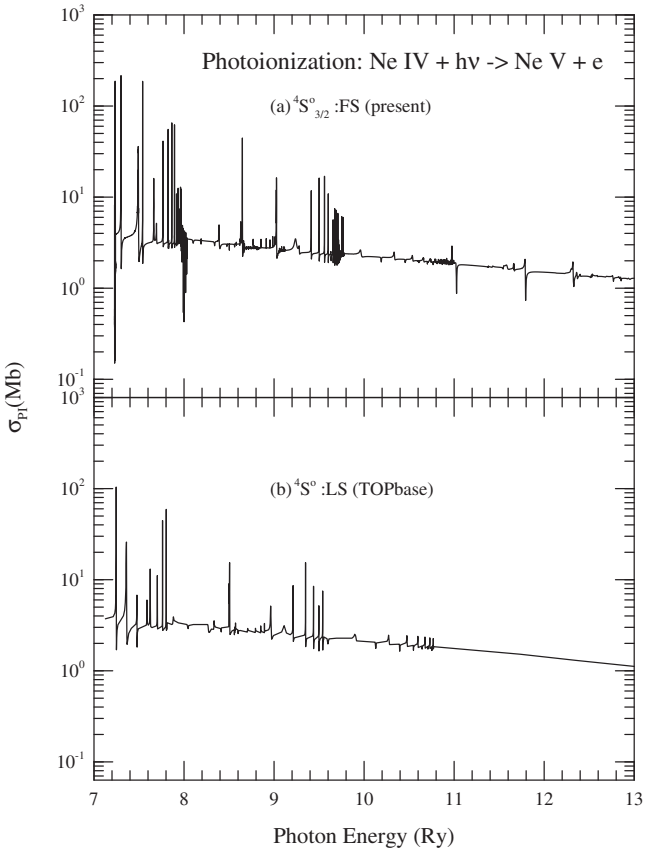

Fig. 1. Photoionization cross sections σ_{PI} of the ground level $1s^22s^22p^3(^4S^o_{3/2})$ of Ne IV: (a) σ_{PI} from present BPRM calculations, (b) σ_{PI} from the TOPbase TOPbase by Lennon and Burke. The cross sections look similar except the resonant structure at the threshold.

codes (Berrington et al., 1995; Nahar and Pradhan, 1994; Zhang et al., 1999). The narrow resonances of photoioniation were delineated at a very fine energy mesh.

4. Results and discussions

Photoionization of Ne IV (Ne IV + $h\nu \rightarrow$ Ne V + e) is studied with detailed resonant features for a large number of bound levels. Present work reports cross sections σ_{PI} of 868 fine structure levels with $n \leqslant 10$ and $l \leqslant 9$ of Ne IV. Important characteristics in σ_{PI} are illustrated below.

The earlier study on photoionization for Ne IV was carried out by Lennon et al. (1993) using R-matrix method in non-relativistic LS coupling approximation and present results for 234 LS states. Results were not published, but the data are available through OP database TOPbase. They considered a close coupling wave function expansion of 10 LS states of core Ne V which is equivalent to the present 20 fine structures levels.

Fig. 1 presents the photoionization cross sections of the ground $1s^22s^22p^3(^4S^o_{3/2})$ level of Ne IV and compares with the earlier total σ_{PI} obtained by Lennon and Burke (TOPbase). The cross section shows relatively smooth background in both panels, typical for a ground ground level, with Rydberg series of resonances. The earlier σ_{PI}, Fig. 1(b), is similar to those in relativistic BPRM calculations except for higher resolution and additional narrow resonances due to fine structure in the present work. For a light and low ionization stage of ion, like Ne IV, relativistic effects are not expected to be

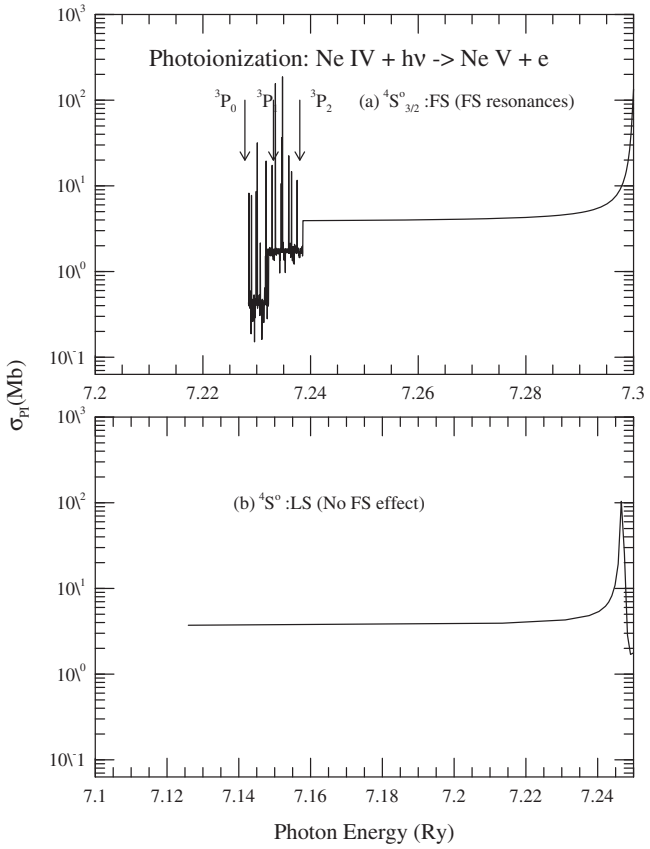

Fig. 2. Photoionization cross sections σ_{PI} of the ground level $1s^22s^22p^3(^4S^o_{3/2})$ of Ne IV in the very low energy region, (a) present BPRM and (b) TOPbase. Resonances in (a) are due to coupling of fine structure channels, not allowed in LS coupling (b). These resonances belong to the Rydberg series of autoionizing states of core levels $1s^22s^22p^2(^3P_1)$ and $1s^22s^22p^2(^3P_2)$. These will have important enhancement effect in the Photoionization as well as recombination rates of Ne IV at very low temperature.

important in general. However, a significant difference in resonant structure is observed at the threshold energy region. The coupling of relativistic fine structure channels has introduced the resonances not allowed in LS coupling.

The expanded fine resolution of these near threshold resonances of the ground level can be seen in Fig. 2. These resonances belong to the Rydberg series of autoionizing states of core levels $1s^22s^22p^2(^3P_1)$ and $1s^22s^22p^2(^3P_2)$ of the ground configuration. The ground state $1s^22s^22p^3(^4S^o)$ can photoionization to ^4P where the state can form from $1s^22s^22p^2(^3P)\epsilon s(^4P)$ or $1s^22s^22p^2(^3P)\epsilon d(^4P)$. In LS coupling $1s^22s^22p^2(^3P)$ is the single ground state and hence has no Rydberg series of resonances. However, in fine structure *jj* coupling, the state has three levels, where ^3P_o is the ground level, $^3P_1$ and $^3P_2$ are the excited levels. Each excited level has series of autoionizing levels, such as, $1s^22s^22p^2(^3P_1)nl$ and $1s^22s^22p^2(^3P_2)nl$ where n is the effective quantum number and l can be s or d. The background jump at $^3P_1$ and $^3P_2$ thresholds at energies 0.0037581 and 0.010116 Ry, respectively beyond the ionization energy 7.23 Ry can be seen clearly. These fine structure resonances will make important contribution to recombination rate coefficient α_{RC} at temperatures 100–1500 K. α_{RC}, which is the Maxwellian average of photoionization, contains the factor $exp(-E/kT)$ where E is photoelectron energy and hence has maximum contribution when energy is zero or almsot zero at and near the ionization threshold. Presence of resonances at and near threshold will increase α_{RC} considerably. This in turn will increase line emissivity and decrease the abundance of the ion (description on the relation can be found, for example in Pradhan and Nahar (2011)).

Relativistic fine structure effect in the low energy region can also be seen in excited states. Fig. 3 illustrates and compares photoionization cross sections of an excited state of Ne IV, $1s^22s2p^4(^2P)$. Although similarities are seen between the present BPRM and earlier LS coupling cross sections. there are additional narrow resonances in fine structure. However, the important difference is the presence of the near threshold resonant structure due to fine structure not formed in LS coupling cross section. The structure from relativistic effects will affect quantities in the low temperature plasmas, such as, photoionization rate Γ of an ion X^{i+}. Γ is given by,

$$\Gamma(s^{-1}) = 4\pi \int_{E_o}^{E_{max}} F(E)\sigma_E dE, \tag{8}$$

where σ_E is the total photoionization cross section in cm^2, $F(E)$ is the photoionizing radiation field, and E_o is the ionization potential of X^{i+}. Near the ground state threshold, as Fig. 2 shows, the LS coupling σ_{PI} lies below 10 Mb while the resonances due to fine structure couplings peak at 10 Mb and above. Hence the rate may enhance by 20–30% at temperature near the ionization threshold.

The other distinct feature in photoionization is the relatively wider Seaton resonances embedded in narrow Rydberg resonances. Seaton resonances, which form due to photo-excitation-of-core (PEC) (Yu and Seaton, 1987), are seen in photoionization of excited levels with single valence electron Fig. 4 presents σ_{PI} of two such excited levels, (a) $1s^22s^22p^23p(^4D^o_{5/2})$, and (b) $1s^22s^22p^24f(^4G^o_{5/2})$ of Ne IV. In the figures, the prominent and wider resonant structures, pointed out by arrows at various energy posi-

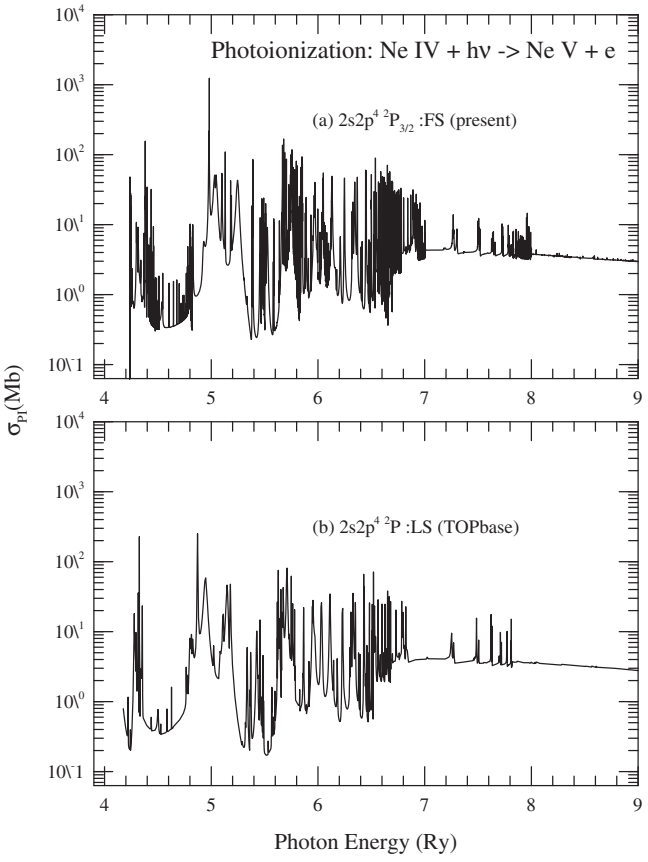

Fig. 3. Photoionization cross sections σ_{PI} of an excited level of Ne IV, $2s2p^4(^2P)$, (a) present BPRM and (b) LS coupling from Lennon and Burke (TOPbase), Distinct resonance at the threshold in (a) is due to relativistic fine structure effect, not allowed in LS coupling.

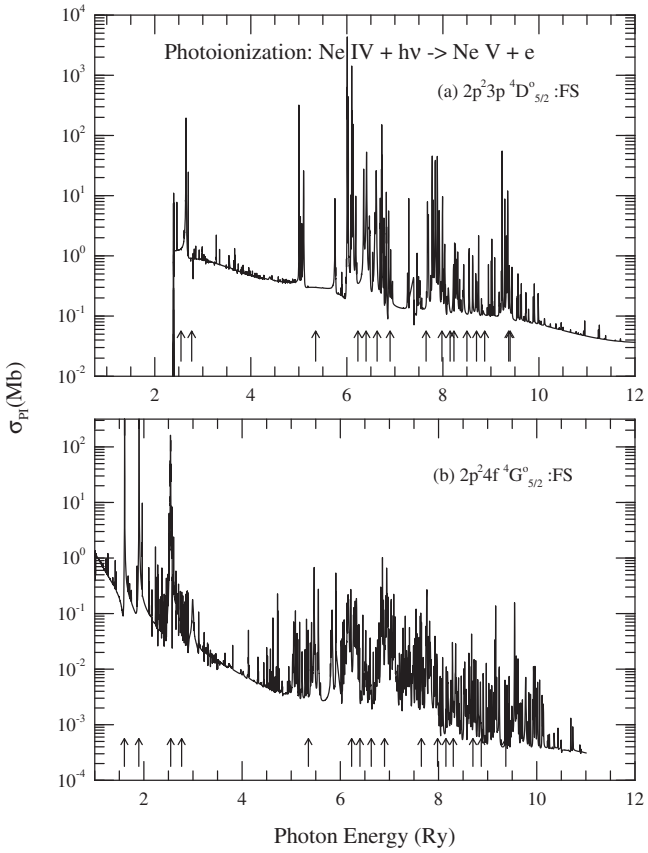

Fig. 4. Photoionization cross sections σ_{PI} of excited levels, (a) $1s^22s^22p^2(^3P)3p(^4D^o_{5/2})$ and (b) $1s^22s^22p^2(^3P)4f(^4G^o_{5/2})$ of Ne IV. Prominent Seaton resonances due to core excitation to various electric dipole allowed levels are indicated by the arrows. These resonances also enhance the background cross section.

Table 2
Photon energies for Seaton resonances in photoionization of excited levels of Ne IV due to core excitation of type $J\pi = 0^e \rightarrow J\pi = 1^o$ from the ground level $1s^2 2s^2 2p^2(^3P_0)$. The configuration number given within parentheses next to each core excited level corresponds to that specified in Table 1.

	Level	J	E(Ry)		Level	J	E(Ry)
1	$^3D^o(2)$	1	1.60	2	$^3P^o(2)$	1	1.90
3	$^3S^o(2)$	1	2.55	4	$^1P^o(2)$	1	2.77
5	$^3P^o(3)$	1	5.35	6	$^3D^o(6)$	1	6.29
7	$^3P^o(6)$	1	6.32	8	$^1P^o(6)$	2	6.41
9	$^5D^o(10)$	1	6.63	10	$^5P^o(10)$	1	6.67
11	$^3D^o(10)$	1	6.82	12	$^3P^o(7)$	1	6.90
13	$^3P^o(10)$	1	7.36	14	$^1P^o(7)$	1	7.40
15	$^3D^o(10)$	1	7.56	16	$^1P^o(10)$	1	7.60
17	$^3P^o(10)$	1	7.65	18	$^1P^o(10)$	1	8.00
19	$^3D^o(10)$	1	8.16	20	$^3P^o(10)$	1	8.22
21	$^3S^o(10)$	1	8.24	22	$^1P^o(10)$	1	8.50
23	$^3S^o(22)$	1	8.70	24	$^3D^o(22)$	1	8.87
25	$^5D^o(24)$	1	9.17	26	$^3P^o(22)$	1	9.28
27	$^3D^o(24)$	1	9.30	28	$^3D^o(24)$	1	9.30
29	$^1P^o(22)$	1	9.40	30	$^3D^o(24)$	1	9.69
31	$^1P^o(24)$	1	9.71	32	$^3P^o(24)$	1	9.74
–	–	–	–	–	$^1P^o(20)$	1	14.18

tions, superimposed on the narrow Rydberg resonances are the illustrative Seaton resonances. These resonances are manifested as the core ground state goes through electric dipole transitions with matching photon energies to these excitations. During excitations the outer electron remains a 'spectator' in a doubly-excited resonant state which decays via autoionization into the ground level of the core and ionization. Hence resonances appear at the core excitation threshold energies for dipole allowed transitions, pointed out by the arrows of some thresholds and listed in Table 2. For example, the core ground level $2s^2 2p^2(^3P_0)$ can be excited to $2s2p^3(^3D^o_1)$ at 1.60 Ry and form Seaton resonance at $^3D^o_1$ threshold, as seen in σ_{PI} for level $2s^2 2p^2(^3P)4f(^4G^o_{5/2})$ Fig. 4(b). It may be noted that, as exemplified in the figure, the positions of these resonance remain at the same energies regardless of the state of the ion. There may be slight variations in positions due to interferences of resonances and one or more resonances may be less distinct or one may not show up in σ_{PI} of low lying excited states. For example, Seaton resonance at threshold $2s^2 2p3s(^3P^o_1)$ at about 5.35 Ry is not visible for level $1s^2 2s^2 2p^2(^3P)3p(^4D^o_{5/2})$ Fig.4(a). However, Seaton resonances become more distinct in photoionization of higher excited levels.

The present BPRM calculations included 20 levels of Ne V which, following Table 1, can have four dipole transition from the ground level $J\pi = 0^e$ to $J\pi = 1^o$ at energies 1.60316 Ry ($^3D^o_1$), 1.89687 ($^3P^o_1$), 2.54576 ($^3S^o_1$), and 2.76854 Ry ($^1P^o$)1) if the ionization threshold lies below them, such as, for $1s^2 2s^2 2p^2(^3P)4f(^4G^o_{5/2})$ Fig. 4(b). However, there are much more Seaton resonances in the high energy region as seen for both levels in Fig. 4. They are generated due to core excitations to higher lying levels. Although 20 levels have been used, the R-matrix code computed all core excitations from the set of 24 configurations given in Table 1 and Seaton resonances were introduced. Positions and strengths of these resonances can be predicted from atomic structure calculations. For the present work, it is found from SS run that these resonances can continue to form up to 14.18 Ry from the 24 configurations. Table 2 lists part of them, about 33 photon energy positions for these resonances. Resonances from closely lying excitations overlap which can further widen the structure and enhance the background. The strength or impact of each resonance will depend on the radiative decay rate of the core excitation.

5. Conclusions

Relativistic BPRM method has been employed, for a complete set of photoiozation for all practical astrophysical and laboratory applications, for one large atomic system of Ne IV. σ_{PI} of a large number of bound levels of Ne IV with $n \leqslant 10$ have been presented. The resonances have been delineated at fine energy mesh. Relativistic fine structure has introduced important resonances at very low energy region, not allowed in LS coupling. This will change the photoionization and recombination rates at temperatures exist in plasmas in planetary nebulae and infra-red galaxies. This will in turn affect the abundance of neon in these objects. Relativistic effects have also introduced denser resonances over the energy range considered in the present work. The present work finds enhanced background cross sections of excited levels of Ne IV by the Seaton resonances formed during dipole allowed core excitations. The present cross sections are expected to be of high accuracy of about 10–15% based on (i) inclusion of relativistic, (ii) higher resolution for resonances, and (iii) consideration of large number configurations.

All photoionization data are available electronically from NORAD-Atomic-Data (NaharOSURadiativeAtomicData) website: <www.astronomy.ohio-state.edu/nahar/nahar_radiativeatomicdata>.

Acknowledgments

This work was supported partially by NSF Astronomy and DOE. The computational work was carried out at the Ohio Supercomputer Center in Columbus Ohio.

References

Berrington, K.A., Burke, P.G., Butler, K., Seaton, M.J., Storey, P.J., Taylor, K.T., Yu, Y., 1987. J. Phys. B 20, 6379.
Berrington, K.A., Eissner, W., Norrington, P.H., 1995. Comput. Phys. Commun. 92, 290.
Burke, P.G., Robb, W.D., 1975. Adv. At. Mol. Phys. 11, 143.
Dance, M., Palay, E., Nahar, S.N., Pradhan, A.K., 2013. MNRAS 435, 1576.
Eissner, W., Jones, M., Nussbaumer, H., 1974. Comput. Phys. Commun. 8, 270.
Houck, J.R. et al., 2004. Astrophys. J. Supp. 154, 18.
Hummer, D.G., Berrington, K.A., Eissner, W., Pradhan, A.K., Saraph, H., Tully, J.A., 1993. Astron. Astrophys. 279, 298.
Lennon D.J., Burke V.M., Lennon D.J. 1993, data available as TOPbase.
Nahar, S.N. ADNDT (submitted 2013).
Nahar, S.N., 2013. J. Quant. Spectrosc. Radiat. Transfer 117, 15.
Nahar, S.N., Pradhan, A.K., 1994. Phys. Rev. A 49, 1816.
Nahar, S.N., Eissner, W., Chen, G.X., Pradhan, A.K., 2003. A&A 408, 789.
Nahar, S.N., Pradhan, A.K., Chen, G.X., Eissner, W., 2011. Phys. Rev. A 83, 053417.
The opacity project team, 1995, 1996. The opacity project, vols. 1–2, Institute of Physics Publishing.
Pradhan, A.K., Nahar, S.N., 2011. Atomic Astrophysics and Spectroscopy. Cambridge University Press.
Rubin, R.H. et al., 2001. ASP Conf. Ser. 247, 479.
Rubin, R.H., 2004. ASP Conference Proceedings of IAU Symposium No. 217, 190.
Seaton, M.J., 1987. J. Phys. B 20, 6363.
The atomic data of the OP is available at TOPbase at <http://cdsweb.u-strasbg.fr/topbase/topbase.html>.
Yu, Y., Seaton, M.J., 1987. J. Phys. B 20, 6409.
Zhang, H.L., Nahar, S.N., Pradhan, A.K., 1999. J. Phys. B 32, 1459.